Revision_1

Albertiniite, $Fe^{2+}(SO_3)\cdot 3H_2O$, a new sulfite mineral species from the Monte Falò Pb-Zn mine, Coiromonte municipality, Verbano Cusio Ossola province, Piedmont, Italy

P. VIGNOLA, G. D. GATTA, N. ROTIROTI, P. GENTILE, F. HATERT, M. BAIJOT, D. BERSANI, A. RISPLENDENTE AND A. PAVESE

Running title: Albertiniite, a new mineral species from Monte Falò, Italy

Abstract

Introduction

Appearance and physical properties

Chemical data

X-ray diffraction data and crystal structure determination

Raman spectroscopy

Acknowledgments

References

List of Tables

Captions of figures

Albertiniite, $Fe^{2+}(SO_3)\cdot 3H_2O$, a new sulfite mineral species from the Monte Falò Pb-Zn mine, Coiromonte municipality, Verbano-Cusio-Ossola province, Piedmont, Italy

P. VIGNOLA[1,2,*], G. D. GATTA[2], N. ROTIROTI[2], P. GENTILE[3], F. HATERT[4], M. BAIJOT[4], D. BERSANI[5], A. RISPLENDENTE[2] AND A. PAVESE[2]

[1]CNR-Istituto per la Dinamica dei Processi Ambientali, via Botticelli 23, I-20133, Milano, Italy.

[2]Dipartimento di Scienze della Terra "A. Desio", Università degli Studi di Milano, via Botticelli 23, I-20133 Milano, Italy.

[3] Dipartimento di Scienze dell'Ambiente e del Territorio e di Scienze della Terra, Università Milano-Bicocca, Piazzale della Scienza 4-building U4, I-20126 Milano, Italy.

[4]Laboratoire de Minéralogie, Département de Géologie, Université de Liège, Bâtiment B18, Sart Tilman, B-4000 Liège, Belgium.

[5]Dipartimento di Fisica e Scienze della Terra, Università di Parma, Viale G.P. Usberti 7/a, I-43124 Parma, Italy

* Corresponding author:

Pietro Vignola

CNR-IDPA, via Botticelli 23, I-20133, Milano, Italy

e-mai: pietro.vignola@idpa.cnr.it; pietroevignola@gmail.com

Abstract

Albertiniite, $Fe^{2+}(SO_3)\cdot 3H_2O$, is a new Fe^{2+} sulfite trihydrated, chemically related to gravegliaite. It occurs at the Monte Falò Pb-Zn mine near Coiromonte, in the Armeno municipality, Verbano-Cusio-Ossola province, Italy. It is an intermediate product of oxidation between iron sulphides and sulphates, forming monoclinic, colourless to pale yellow transparent crystals with vitreous lustre. The mineral occurs associated with stolzite, pyromorphite, hinsdalite, plumbogummite, gibbsite, scheelite, and jarosite on brittle fractures of quartz veins or chlorite-schist. Albertiniite is optically biaxial positive (+) with $2V_{(meas)} \sim 40°$ and $2V_{(calc)} = 66°$. The measured refractive indices, using sodium light (589 nm), are: $\alpha = 1.612(2)$ °, $\beta = 1.618(2)$ °, and $\gamma = 1.632(2)$ °. The optical axis plane is parallel to the perfect {010} cleavage plane. It is non fluorescent under short-wave (254 nm) or long-wave (366 nm) ultraviolet light. The calculated density is 2.469 g/cm^3 (from the crystal-structure refinement), or 2.458 g/cm^3 (from the chemical analysis and the single-crystal unit-cell parameters). The empirical formula is (average of 16 spots and based on 3 anhydrous oxygen a.p.f.u.) : $(Fe^{2+}_{0.774}Mn^{2+}_{0.282}Ca_{0.001}Mg_{0.001}Na_{0.003})_{\Sigma 1.061}(S_{0.971}O_3)\cdot 2.84H_2O$, with the H_2O content calculated by difference to 100 wt%. Albertiniite is monoclinic with space group $P2_1/n$. Its unit-cell parameters are: $a = 6.633(1)$ Å, $b = 8.831(1)$ Å, $c = 8.773(1)$ Å, $\beta = 96.106(8)$ ° and $V = 511.0(1)$ Å^3,with Z = 4. The eight strongest measured lines in the X-ray powder diffraction pattern are [d in Å, (I/I_0), (hkl)]: 4.072 (100) (-111), 3.539 (93) (-112), 5.533 (27) (-101), 6.167 (14) (011), 2.830 (14) (211), 4.998 (14) (101), 4.353 (12) (111), and 3.897 (12) (012). The mineral, which has been approved by the CNMNC under number IMA2015-004, is named albertiniite in honour of Claudio Albertini, an Italian mineral collector expert in the systematic mineralogy of Alps and pegmatites.

KEYWORDS: albertiniite, Fe sulfite trihydrated, Monte Falò Pb-Zn mine, Verbania province, Italy.

Introduction

Mineral species belonging to the sulfite subgroup, oxide class in the classification of Strunz (Strunz and Nickel, 2001), are very rare in nature. The four known species belonging to this subgroup are gravegliaite, $Mn^{2+}(SO_3)\cdot3H_2O$, hannebachite, $Ca(SO_3)\cdot H_2O$, scotlandite, $Pb(SO_3)$, and the sulphate-sulfite orschallite, $Ca_3(SO_3)_2(SO_4)\cdot12H_2O$. Gravegliaite and scotlandite can be considered as intermediate products of the oxidation process which transforms oxides and sulphides into sulphates, where hannebachite and orschallite crystallize in a moderately oxidizing hydrothermal environment. Hannebachite and orschallite were found and described for the first time in the magmatic rocks of the Eifel volcanic area (Palatinate, Germany) (Hentschel *et al.*, 1985; Weidenthaler *et al.*, 1993). Scotlandite, more common in respect of the other three species, was described for the first time at the Susanna lead mine, Leadhills, Scotland (Paar *et al.*, 1984), as a product of oxidation of galena and Pb-sulphides. Gravegliaite was described as the product of oxidation of the braunite + hausmannite + tephroite mineralization at the Gambatesa Mn-mine, Val Graveglia, Italy, as micro-crystals along fractures in the Mn-mineralization (Basso *et al.*, 1991). Albertiniite is an iron sulfite trihydrated, chemically related to gravegliaite. The mineral and its name had been approved by the IMA Commission on New Minerals, Nomenclature and Classification (IMA2015-004, Vignola *et al.*, 2015). The mineral is named in honour of Claudio Albertini, an Italian mineral collector expert in the systematic mineralogy of Alps and pegmatites. Claudio Albertini is author of several papers on the principal journals for mineral collectors and scientists, and he is author of the volume "*L'Alpe Devero e i suoi minerali*" on the worldwide famous locality of Mount Cervandone. Claudio found, and proposed to the scientific community, two new mineral species: fetiasite (Graeser *et al.*, 1994), albertiniite (present work), and a new phase still under investigation.

The co-type samples used for the complete characterization of the new species albertiniite are deposited in the Mineralogical Collection of the Museo Civico di Storia Naturale, Milano, Italy, (Fig. 1)(number MM 38728; co-type used for chemical analysis, paragenesis description, X-ray powder diffraction, Raman spectroscopy), and in the collection of the Laboratory of Mineralogy, University of Liège, Belgium (number 20393; co-type used for optical measurements and single-crystal X-ray structure determination).

Appearance and physical properties

Albertiniite was found by Claudio Albertini on 2010 at the mine dumps at the Monte Falò Pb-Zn mine near Coiromonte, in the Armeno municipality, Verbano-Cusio-Ossola province, Italy (latitude 45°50'52.37"N - longitude 8°29'1.13"E). The mine was active in the period 1920 - 1953 and the tunnels (now collapsed) reached a total length of about 340 m. Galena was the most important mined mineral, with minor sphalerite, arsenopyrite, pyrite and marcasite (Albertini *et al*., 2014). The ore is constituted by the aforementioned sulphides hosted by quartz veins embedded in a chlorite-rich micaschist, characterized by an unusual secondary minerals association given by stolzite, pyromorphite, hinsdalite, plumbogummite, gibbsite, scheelite, jarosite, and albertiniite (mostly covered by an amorphous hydrated iron oxide). The mineral occurs on the surfaces of brittle fractures in quartz veins and in the chlorite-schist hosting the mineralized quartz veins, in monoclinic prisms up to 0.7 mm across, sometimes showing rounded corners and edges. Albertiniite crystals are frequently covered by brownish amorphous hydrated Fe-oxides, probably pseudomorphs after a mineral with a rhombohedral shape (Fig. 2). The mineral shows, under the polarizing microscope, a perfect {010} cleavage, it is brittle with an irregular fracture. The new species forms colorless to yellowish (under natural light), transparent crystals with a vitreous lustre. It is biaxial positive (+), with $2V_{(meas)} \sim 40°$ and $2V_{(calc)} = 66°$. The measured refractive indexes, using sodium light (589 nm), are: $\alpha = 1.612(2)$ °, $\beta = 1.618(2)$ °, and $\gamma = 1.632(2)$ °. The optical axis plan is parallel to the perfect {010} cleavage plane. The mineral is colourless and non pleochroic under polarized light. Due to the scarcity of crystals, the density was not measured. The calculated density is 2.469 g/cm^3 (from the crystal-structure refinement), or 2.458 g/cm^3 (from the chemical analysis and the single-crystal unit-cell parameters).

The compatibility index is 0.012, if calculated with the density obtained from crystal structure data, or 0.008, if calculated with the density obtained from the chemical data. For the compatibility calculations, we used the K_i constants calculated for oxides by Mandarino (1981) (SO_2, FeO, MnO, CaO, MgO, Na_2O, and H_2O).

Chemical data

Preliminary chemical data, along with secondary-electron and back-scattered images of albertiniite, were collected both on natural samples and polished sections by a Tescan Vega TS 5136 XM scanning electron microscope (SEM) equipped with an EDAX Genesis 4000 JXM energy dispersive spectrometer (EDS), at the "Centro interdipartimentale di microscopia elettronica" of the University of Milano-Bicocca.

Quantitative chemical analyses were then performed on the polished sections using a JEOL JXA-8200 electron microprobe in wavelength-dispersive mode at the laboratory of the Earth Sciences Department, University of Milano (ESD-MI). The system was operated using an accelerating voltage of 15 kV, a beam current of 5 nA, a spot size of 15 µm, and a counting time of 30 sec on the peaks and 10 sec on the background. Grossular for Si ($K\alpha$) and Ca ($K\alpha$), celestine for S ($K\alpha$), omphacite for Na ($K\alpha$), fajalite for Fe ($K\alpha$), rhodonite for Mn ($K\alpha$), forsterite for Mg ($K\alpha$), K-feldspar for K ($K\alpha$), graftonite for P ($K\alpha$), realgar for As ($L\alpha$) and cancrinite for Cl ($K\alpha$) served as standards. The raw data were corrected for matrix effects using the ϕρZ method from the JEOL series of programs. The following elements were below detection limit in all 16 microprobe spots: Si, P, Al, K, and Cl. The mean analytical results are reported in Table 1. H_2O was not determined directly, due to the small amount of material, and was calculated by difference to 100 wt%. The empirical formula calculated on the basis of 3 anhydrous oxygen atoms per formula unit (a.p.f.u.) is: $(Fe^{2+}_{0.774}Mn^{2+}_{0.282}Ca_{0.001}Mg_{0.001}Na_{0.003})_{\Sigma 1.061}(S_{0.971}O_3)\cdot 2.84H_2O$. The simplified formula is $Fe^{2+}(SO_3)\cdot 3H_2O$, which requires: SO_2 = 33.73 wt%, FeO = 37.82 wt%, and H_2O = 28.45 wt% for a total of 100.00 wt%.

X-ray diffraction data and crystal structure refinement

The X-ray powder diffraction (XRPD) pattern of albertiniite was collected by a high-resolution Panalytical X'pert Pro X-ray powder diffractometer equipped with a X'Celerator-type detector at the ESD-MI. Operating conditions were: Ni-filtered Cu*K*α radiation, 40 kV, 40 mA, 2θ-range from 5° to 120°, step size of 2θ = 0.017°, and a counting time of 300 s per step. The refinement of unit-cell parameters were performed using the program CELREF 3 (Laugier and Bochu, 1999), based on the structure model obtained by single-crystal X-ray diffraction (see below). Silicon NIST 640c was used as line-position internal standard. The reflection conditions were found to be consistent with the space group $P2_1/n$. The refined unit-cell parameters are: a = 6.633(10) Å, b = 8.831(9) Å, c = 8.771(13) Å, β = 96.2(2)º, and V = 511(1) Å^3 (with Z = 4). The complete list of indexed reflections is reported in Table 2. The eight strongest measured lines are [*d* in Å, (I/I_0), (*hkl*)]: 4.072 (100) (-111), 3.539 (93) (-112), 5.533 (27) (-101), 6.167 (14) (011), 2.830 (14) (211), 4.998 (14) (101), 4.353 (12) (111), and 3.897 (12) (012).

Single-crystal X-ray diffraction data were collected with an Xcalibur - Oxford Diffraction diffractometer equipped with a CCD, using graphite-monocromatized Mo*K*α radiation and operated at 50 kV and 40 mA at the ESD-MI. To maximize the reciprocal space coverage, a combination of ω and ϕ scans was used, with a step size of 1° and an exposure time per frame of 10 s. A total number of 14415 reflections up to $2\theta_{max}$ of 72.3° were collected, out of which 1668 were unique, giving a metrically monoclinic unit-cell with: a = 6.633(1) Å, b = 8.831(1) Å, c = 8.773(1) Å, β = 96.106(8) ° and V = 511.0(1) Å^3 (Table 3). The reflections conditions suggested the space group $P2_1/n$ as highly likely.

The X-ray intensity data were first processed with the programs E-STATISTICS, implemented in the WinGX package (Farrugia, 1999). The statistics of distributions of the normalized structure factors (*E*'s) showed, unambiguously (~ 70% likelihood), that the structure is centrosymmetric. The anisotropic structure refinement was then performed in the space group $P2_1/n$ using the SHELX-97 software (Sheldrick 1997, 2008), starting from the site coordinates of the synthetic α-$Fe^{2+}(SO_3)\cdot3H_2O$ reported by Johansson and Lindqvist (1979), in which the H sites were not located. The neutral X-ray scattering curves of Fe, Mn, S, O and H were used according to the International Tables for Crystallography *C* (Wilson and Prince, 1999). The secondary isotropic extinction effect was modelled according to the Larson's formalism (Larson, 1967), as implemented in the SHELXL-97 package (Sheldrick 1997, 2008), though the refined value of the extinction coefficient was not significant. The octahedral *M* site was first modelled with a mixed (Fe + Mn) scattering curve according to the chemical analysis (Tables 1 and 4); however, this did not improve the figure of merit of the refinement with respect to the site fully populated by Fe. Six independent H sites were added to the structure model on the basis of the maxima found in the difference-Fourier map of the electron density. The relative O-H distances were restrained to a target value of 0.95 ± 0.03 Å. The convergence was rapidly achieved and the variance-covariance matrix showed no high correlation among the refined parameters; the six H sites were refined isotropically, with a restrained group value (Table 4). No peaks larger than +/- 0.5 e-/$Å^3$ were present in the final difference-Fourier maps of the electron density (Table 3). The final agreement index (R_1) was 0.0227 for 92 refined parameters and 1409 unique reflections with $Fo>4\sigma(Fo)$ (Table 3). Atomic coordinates and displacement parameters are reported in Table 4. Relevant bond lengths and angles are listed in Table 5.

Raman spectroscopy

Single-crystal Raman spectrum of albertiniite was collected using an Olympus BX40 microscope attached to a Jobin-Yvon Horiba LabRam confocal Raman spectrometer, equipped with a charge-coupled detector (CCD), at the University of Parma. The spectrum was collected exciting the sample with the 473.1 nm laser light. The laser beam was focused on the sample on a spot with nearly 2 μm of diameter (objective 50x) and the confocal aperture was set at 150 μm. The Raman spectrum was collected in backscattered geometry, in the spectral range 100 - 4000 cm^{-1}, with 200 s counting time and 3 accumulations (Fig. 3 and 4). The position of the Raman bands was measured using a Gauss-Lorentzian de-convolution procedure with the LabSpec v.5 software, with a precision of 0.5 cm^{-1}. The wavenumbers of the Raman bands are reported in Table 6.

Discussion

The new mineral albertiniite is the product of the intermediate oxidation of Fe sulphides (*e.g.*, pyrite, arsenopyrite) in a Ca-rich hydrothermal environment. Albertiniite is a (Fe^{2+}, Mn)-sulfite trihydrated chemically related to gravegliaite, Strunz 4.JE.05, Dana 34.2.05.2. It corresponds to the monoclinic Fe-equivalent of gravegliaite, ideally $Mn^{2+}(SO_3)\cdot 3H_2O$ (Basso *et al.*, 1991; Table 7). The comparison between the crystallographic features of albertiniite and those of its synthetic counterpart α-$FeSO_3\cdot 3H_2O$, gravegliaite and the synthetic $MnSO_3\cdot 3H_2O$ are given in Table 7. Among those, the Mn-dominant minerals have orthorhombic structures (as observed in gravegliaite and synthetic $MnSO_3\cdot 3H_2O$), whereas the Fe-dominant albertiniite and α-$FeSO_3\cdot 3H_2O$ structures are monoclinic (Table 7).

A view of the crystal structure of albertiniite is shown in Fig. 5. Each Fe atom is 6-fold coordinated to three different sulfite O atoms and three H_2O molecules, giving a slightly distorted octahedron (the difference between the longest and the shortest *M*-O distances is ~0.17 Å, Table 5). The sulfite group shows S-O bond distances similar to those previously reported for the synthetic α-$FeSO_3\cdot 3H_2O$, with S-O1 > S-O3 > S-O2 (Johansson and Lindqvist, 1979; Table 5). Each sulfite ion is bonded to three Fe atoms, giving a three-dimensional net of Fe-O-S interactions. The H-bonding scheme in albertiniite is the following: O1···H2-O6-H1···O4, O3···H4-O5-H3···O2, and O6···H6-O4-H5···O1 (Table 5). All the H-bonds show O-H···O angles > 160°and H···O distances ≤ 2 Å(Table 5).

The Raman spectrum of albertiniite (Fig. 3 and 4, Table 6) is typical of a hydrate sulfite, containing the stretching (*i.e.*, 3215 and 3350 cm^{-1}, Table 6) and bending (*i.e.*, 1660 cm^{-1}, Table 6) modes of H_2O, along with stretching and bending modes of the pyramidal SO_3^{2-} ion (observed between 438 and 970 cm^{-1}, Table 6). The free SO_3^{2-} is expected to show only 4 Raman modes, while in a crystal structure the local distortion of the pyramid will remove the double degeneracy of the asymmetric modes ν_3 and ν_4, leading to a total of 6 modes. Here we observe a total of 11 modes that can be ascribed to SO_3^{2-} (Table 6). For any given oxygen atom (O_j) belonging to the coordination environment of the octahedral site, the presence of Mn and Fe (co-sharing the *M* site) leads to slightly different *M*-O_j distances at the local scale, which, in turn, will give different S-O_j distances. We are inclined to consider the doubling of the Raman active modes of the SO_3^{2-}group as the effect of local Fe/Mn ordering.

Acknowledgments

The authors are grateful to Claudio Albertini for having provided the new mineral of this study. The authors are particularly grateful to P. Leverett, Jakub Plášil and an anonymous reviewer, and to the Editors P. Williams and S. Mills for their constructive comments.

References

Albertini, C., Bertolotti, G. P., Grassi V., Gruppo Grotte Novara, Lana, E., Manni, C. and Montrasio, A. (2014) Miniere e minerali del Vergante e Val d'Agogna. Gruppo Archeologico, Storico, Mineralogico Aronese (G.A.S.M.A.) Editor, Arona (VB), Italy.

Baggio, R.F. and Baggio, S. (1976) Chrystal structure and chemical bonding of manganese (II) sulphite trihydrate. *Acta Crystallographica*, **B32**, 1959-1962.

Basso, R., Lucchetti, G. and Palenzona, A. (1991) Gravegliaite, $MnSO_3{\cdot}3H_2O$, a new mineral from Val Graveglia (Northern Appennines, Italy). *Zeitschrift für Kristallographie*, **197**, 97-106.

Farrugia, L.J. (1999) WinGX suite for small-molecule single-crystal crystallography. *Journal of Applied Crystallography*, **32**, 837-838.

Graeser, S., Schwander, H., Demartin, F., Gramaccioli, C.M., Pilati, T. and Reusser, E. (1994) Fetiasite $(Fe^{2+},Fe^{3+},Ti)_3O_2[As_2O_5]$, a new arsenite mineral; its description and structure determination. *American Mineralogist*, **79**, 996-1002.

Hentschel, G., Tillmanns, E. and Hofmeister, W. (1985): Hannebachite, natural calciumsulfite hemihydrate, CaS03.1/2H2O. *Neues Jahrbuch für Mineralogie Monatshefte*, **1985**, 241-250.

Johansson, L.G. and Lindquist, O. (1979) The crystal structure of iron (II) sulfite trihydrate, α-$FeSO_3{\cdot}3H_2O$. *Acta Crystallographica*, **B35**, 1017-1020.

Larson, A.C. (1967) Inclusion of secondary extinction in least-squares calculations. *Acta Crystallographica*, **23**, 664 – 665.

Laugier, J. and Bochu, B. (1999) – CELREF: Cell parameters refinement program from powder diffraction diagram – Laboratoire des Matériaux et du Génie Physique, Ècole Nationale Supérieur de Physique de Grenoble (INGP), Grenoble, France.

Mandarino, J.A. (1981): The Gladstone-Dale relationship: Part IV. The compatibility concept and its application. *Canadian Mineralogist,* **19**, 441-450.

Paar, W. H., Braithwaite, R. S. W., Chen, T. T. and Keller, P. (1984) A new mineral, scotlandite (PbSO3) from Leadhills, Scotland; the first naturally occurring sulfite. *Mineralogical Magazine*, **48**, 283-288.

Sheldrick, G.M. (1997) SHELX-97 – A program for crystal structure refinement. University of Göttingen, Göttingen.

Sheldrick, G.M. (2008) A short history of SHELX. *Acta Crystallographica*, **A64**, 112-122.

Strunz H and Nickel E.H. (2001) Strunz mineralogical tables. 9th Edition, E. Schweizerbart'sche Verlagbuchhandlung, Stuttgart, Detusheland.

Vignola, P., Gatta, G.D., Rotiroti, N., Gentile, P., Hatert, F., Baijot, M., Bersani, D., Risplendente, A. and Pavese, A. (2015) Albertiniite, IMA 2015-004. CNMNC. Newsletter No. 25, June 2015, page xxx; *Mineralogical Magazine*, (in press).

Weidenthaler, C., Tillmanns, E. and Hentschel, G. (1993) Orschallite, $Ca_3(SO_3)_2SO_4*12H_2O$, a new calcium-sulfite-sulfate-hydrate mineral. *Mineralogy and Petrology*, **48**, 167-177.

Wilson, A.J.C. and Prince, E. (1999) International Tables for Crystallography Vol. C, Mathematical, Physical and Chemical Tables, second ed., Kluwer, Dordrecht.

LIST OF TABLES

CAPTIONS OF FIGURES

Figure 1. Albertiniite, crystal of 0.4 mm x 0.25 mm from Monte Falò. Co-type specimen at the Museum of Natural History of Milano (catalogue # 38728).

Figure 2. Back-scattered electron image of albertiniite from Monte Falò.

Figure 3. The un-polarised Raman spectra of albertiniite.

Figure 4. The un-polarised Raman spectra of albertiniite from 100 to 1100 cm^{-1}.

Figure 5. The crystal structure of albertiniite based on the structure refinement of this study. Thermal ellipsoid probability factors: 50%.

Table 1. Electron microprobe analysis of albertiniite

	wt% *	e.s.d.	range		*a.p.f.u.***
SO_2	32.88	0.77	(31.54-33.95)	S	0.971
FeO	29.38	1.89	(24.29-32.40)	Fe^{2+}	0.774
MnO	10.58	1.47	(8.60-14.46)	Mn^{2+}	0.282
CaO	0.02	0.01	(0.01-0.04)	Ca	0.001
MgO	0.01	0.02	(0.00-0.08)	Mg	0.001
Na_2O	0.05	0.03	(0.00-0.09)	Na	0.003
H_2O	27.07			OH^-	2.84
Total	100				

Notes: * average of 16 analyses; ** calculated on the basis of 3 (non-H_2O) oxygen a.p.f.u.; H_2O by difference to 100 wt%.

Table 2. Powder X-ray diffraction data of albertiniite

I/I_0	d_{obs}	d_{calc}	*h k l*
14	6.167	6.205	0 1 1
27	5.533	5.554	-1 0 1
11	5.257	5.284	1 1 0
14	4.998	5.008	1 0 1
100	4.721	4.702	-1 1 1
12	4.353	4.356	1 1 1
12	3.897	3.909	0 1 2
93	3.539	3.515	-1 1 2
10	3.29	3.297	2 0 0
10	3.076	3.089	2 1 0
9	2.994	3.008	-2 1 1
7	2.873	2.894	-1 2 2
14	2.83	2.824	2 1 1
8	2.759	2.761	0 1 3
4	2.23	2.232	-2 1 3
4	2.183	2.18	0 0 4
4	2.169	2.166	-2 3 1
6	2.115	2.116	0 1 4
5	2.022	2.02	1 4 1
3	2.003	2	-3 1 2
3	1.912	1.913	-1 4 2
4	1.873	1.872	-2 1 4
3	1.862	1.863	1 4 2
2	1.819	1.817	-2 4 1
2	1.665	1.666	1 5 1
3	1.416	1.416	-2 3 5
2	1.413	1.412	4 2 2

Table 3. Details about the single-crystal X-ray data collection and structure refinement of albertiniite

Crystal shape	Irregular prism
Crystal size (mm^3)	0.180 x 0.150 x 0.090
Crystal color	Transparent, colorless
T (K)	298
Unit-cell constants	a = 6.633 (1) Å
	b = 8.831 (1) Å
	c = 8.773 (1) Å
	β = 96.106 (8) °
	V = 511.0 (1) $Å^3$
Reference chemical formula	$Fe^{2+}(SO_3)\cdot 3H_2O$
Space Group	$P2_1/n$
Z	4
Radiation (Å)	Mo$K\alpha$
Diffractometer	Xcalibur - CCD
Data-collection method	ω/φ scan
Step size (°) / Time per frame (s)	1 / 10
Max. θ (°)	72.33
	$-8 < h < 8$
	$-14 < k < 14$
	$-13 < l < 14$
No. measured reflections	14415
No. unique reflections	1668
No. unique refl. with $F_o > 4\sigma(F_o)$	1409
No. refined parameters	92
Refinement on	F^2
R_{int}	0.0339
R_1 (F) with $F_o > 4\sigma(F_o)$	0.0227
R_1 (F) for all the unique reflections	0.0342
$wR_2\,(F^2)$	0.0429
GooF	1.657
Weighting scheme: a, b	0.01, 0
Residuals (e^-/ $Å^3$)	+0.504 / -0.494

$R_{int} = \Sigma \mid F_{obs}^2 - F_{obs}^2(\text{mean}) \mid / \Sigma [F_{obs}^2]$; $R_1 = \Sigma(|F_{obs}| - |F_{calc}|)/\Sigma|F_{obs}|$;

$wR_2 = [\Sigma[w(F^2_{obs} - F^2_{calc})^2]/\Sigma[w(F^2_{obs})^2]]^{0.5}$, $w = 1/ [\sigma^2(F_{obs}^2) + (a{*}P)^2 + b{*}P]$,

$P = (\text{Max}\ (F_{obs}^2, 0) + 2{*}F_{calc}^2)/3$

Table 4. Refined fractional coordinates and displacement parameters (Å^2)in the expression: $-2\pi^2[(ha^*)^2U_{11} + \ldots + 2hka^*b^*U_{12} + \ldots + 2klb^*c^*U_{23}]$.$U_{\mathrm{eq}}$ is defined as one third of the trace of the orthogonalisedU_{ij}tensor.

Site	x	y	z	U_{11}	U_{22}	U_{33}	U_{23}	U_{13}	U_{12}	$U_{\mathrm{eq./iso}}$
M	0.42944(4)	0.24709(2)	0.14459(2)	0.0124(1)	0.01203(9)	0.01331(11)	0.00146(8)	0.00112(9)	0.00001(9)	0.0126(1)
S	0.82444(6)	0.07021(4)	0.32605(4)	0.0088(1)	0.0135(1)	0.0118(2)	-0.0004(1)	0.0019(1)	-0.0001(1)	0.0113(1)
O1	0.9551(2)	0.1986(1)	0.4052(1)	0.0150(7)	0.0193(5)	0.0151(5)	-0.0058(4)	0.0015(5)	-0.0027(5))	0.0165(2)
O2	0.7224(2)	0.1429(1)	0.1794(1)	0.0142(7)	0.0242(5)	0.0157(5)	-0.0006(4)	-0.0025(5)	0.0074(5)	0.0183(2)
O3	0.5211(2)	0.4623(1)	0.2333(1)	0.0175(7)	0.0124(5)	0.0197(5)	-0.0005(4)	0.0041(5)	-0.0040(4)	0.0164(2)
O4	0.1117(2)	0.3475(1)	0.1431(1)	0.0144(7)	0.0156(5)	0.0183(5)	0.0006(4)	0.0010(5)	-0.0004(5)	0.0161(2)
O5	0.2667(2)	0.0461(1)	0.0742(1)	0.0301(8)	0.0224(6)	0.0177(6)	-0.0066(4)	0.0071(5)	-0-0098(6)	0.0231(3)
O6	0.3613(19)	0.1682(1)	0.3745(1)	0.0127(7)	0.0244(6)	0.0119(5)	0.0013(5)	0.0001(5)	0.0001(5)	0.0164(2)
H1	0.454(3)	0.181(3)	0.461(2)							0.050(3)
H2	0.234(2)	0.174(3)	0.403(2)							0.050(3)
H3	0.270(3)	-0.002(2)	-0.018(1)							0.050(3)
H4	0.157(2)	0.023(2)	0.128(2)							0.050(3)
H5	0.034(3)	0.311(3)	0.216(2)							0.050(3)
H6	0.115(3)	0.453(1)	0.145(2)							0.050(3)

Note: The M site was modelled with the scattering curve of Fe;$U_{\mathrm{iso}}(\mathrm{H1})=U_{\mathrm{iso}}(\mathrm{H2})=U_{\mathrm{iso}}(\mathrm{H3})=U_{\mathrm{iso}}(\mathrm{H4})=U_{\mathrm{iso}}(\mathrm{H5})=U_{\mathrm{iso}}(\mathrm{H6})$.

Table 5. Refined bond distances (Å) and angles (°)

M-O1	2.178(1)	O1-M-O2	93.99(4)
M-O2	2.143(1)	O1-M-O3	96.19(4)
M-O3	2.118(1)	O1-M-O4	94.32(4)
M-O4	2.285(1)	O1-M-O5	89.62(4)
M-O5	2.134(1)	O1-M-O6	170.97(4)
M-O6	2.222(1)	O2-M-O3	96.45(4)
		O2-M-O4	171.66(4)
S-O1	1.546(1)	O2-M-O5	96.16(5)
S-O2	1.529(1)	O2-M-O6	90.00(4)
S-O3	1.530(1)	O3-M-O4	83.25(4)
		O3-M-O5	165.70(5)
O6-H1	0.93(2)	O3-M-O6	91.40(4)
H1···O4	1.83(2)	O4-M-O5	83.29(5)
O6···O4	2.73(1)	O4-M-O6	81.68(4)
O6-H1···O4	164(1)	O5-M-O6	81.89(4)
O6-H2	0.92(1)	O1-S-O2	104.29(6)
H2···O1	1.86(1)	O1-S-O3	104.25(7)
O6···O1	2.76(1)	O2-S-O3	103.14(6)
O6-H2···O1	164(1)		
H1-O6-H2	108(2)		
H3-O5-H4	116(2)		
O5-H3	0.92(2)	O5-H4	0.93(2)
H3···O2	1.89(2)	H4···O3	1.86(2)
O5···O2	2.79(1)	O5···O3	2.78(1)
O5-H3···O2	167(1)	O5-H4···O3	168(2)
H5-O4-H6	110(2)		
O4-H5	0.92(2)	O4-H6	0.93(1)
H5···O1	2.05(2)	H6···O6	1.92(1)
O4···O1	2.93(1)	O4···O6	2.84(1)
O4-H5···O1	161(2)	O4-H6···O6	173(1)

Table 6. Wavenumber of the Raman bands measured in albertiniite and their assignments

Wavenumber (cm^{-1})	*Int.*	*Assignment*
123	m	Lattice mode
172		Lattice mode
197	w	Lattice mode
241	w	Lattice mode
279	w	Lattice mode
324	w,b	Lattice mode
438	w,sh	ν_4 SO_3 (asymmetric bending)
457	m	ν_4 SO_3 (asymmetric bending)
482	m	ν_4 SO_3 (asymmetric bending)
495	sh	ν_4 SO_3 (asymmetric bending)
600	w,b	ν_2 SO_3 (symmetric bending)
660	w,b	ν_2 SO_3 (symmetric bending)
825	w	ν_3 SO_3 (asymmetric stretching)
860	w	ν_3 SO_3 (asymmetric stretching)
910	m	ν_3 SO_3 (asymmetric stretching)
950	s	ν_3 SO_3 (asymmetric stretching)
970	vs	ν_1 SO_3 (symmetric stretching)
1660	w	O-H- O bending (H_2O)
3215	vs	OH stretching (H_2O)
3350	vs	OH stretching (H_2O)

Table 7. Comparison between the crystallographic features of albertiniite with gravegliaite and the synthetic analogues.

Mineral	albertiniite	Synthetic α-$FeSO_3\cdot 3H_2O$	gravegliaite	synthetic $MnSO_3\cdot 3H_2O$
Reference	This work	[1]	[2]	[3]
Ideal formula	$Fe^{2+}(SO_3)\cdot 3H_2O$	$Fe^{2+}(SO_3)\cdot 3H_2O$	$Mn^{2+}(SO_3)\cdot 3H_2O$	$Mn^{2+}(SO_3)\cdot 3H_2O$
Crystal system	monoclinic	monoclinic	orthorhombic	orthorhombic
Space group	$P2_1/n$	$P2_1/n$	*Pnma*	*Pnma*
a (Å)	6.633(1)	6.604(2)	9.763(1)	9.72(2)
b (Å)	8.831(1)	8.693(1)	5.635(1)	5.63(1)
c (Å)	8.773(2)	8.714(2)	9.558(1)	9.53(2)
β (°)	96.106(8)	96.05(2)		
Z	4	4	4	4
Strong X-ray lines	6.167 (14)	5.522 (M)	6.83(S)	—
	5.533 (27)	4.661 (S)	4.33(VS)	—
	5.257 (11)	3.878 (S	3.43(VS)	—
	4.998 (14)	3.277 (S)	2.704(M)	—
	4.721 (100)	3.072 (M)	2.666(M)	—
	4.353 (12)	2.863 (M)	2.414(M)	—
	3.897 (12)	2.753 (M)	1.726(M)	—
	3.539 (93)	2.220 (M)	—	—
	3.290 (10)	1.939 (M)	—	—
	2.830 (14)	1.870 (M)	—	—
Density	2.469 (calc.)	—	2.39 (calc.)	2.40 (meas), 2.40 (calc)
Color	Colorless, pale yellow transparent	Pale green, transparent	Colorless, transparent	Colorless, transparent
Morphology	Prismatic		Prismatic {*010*}	Prismatic {*010*}

[1] Johansson and Lindquist (1979), [2] Basso *et al.* (1991), [3] Baggio and Baggio (1976).

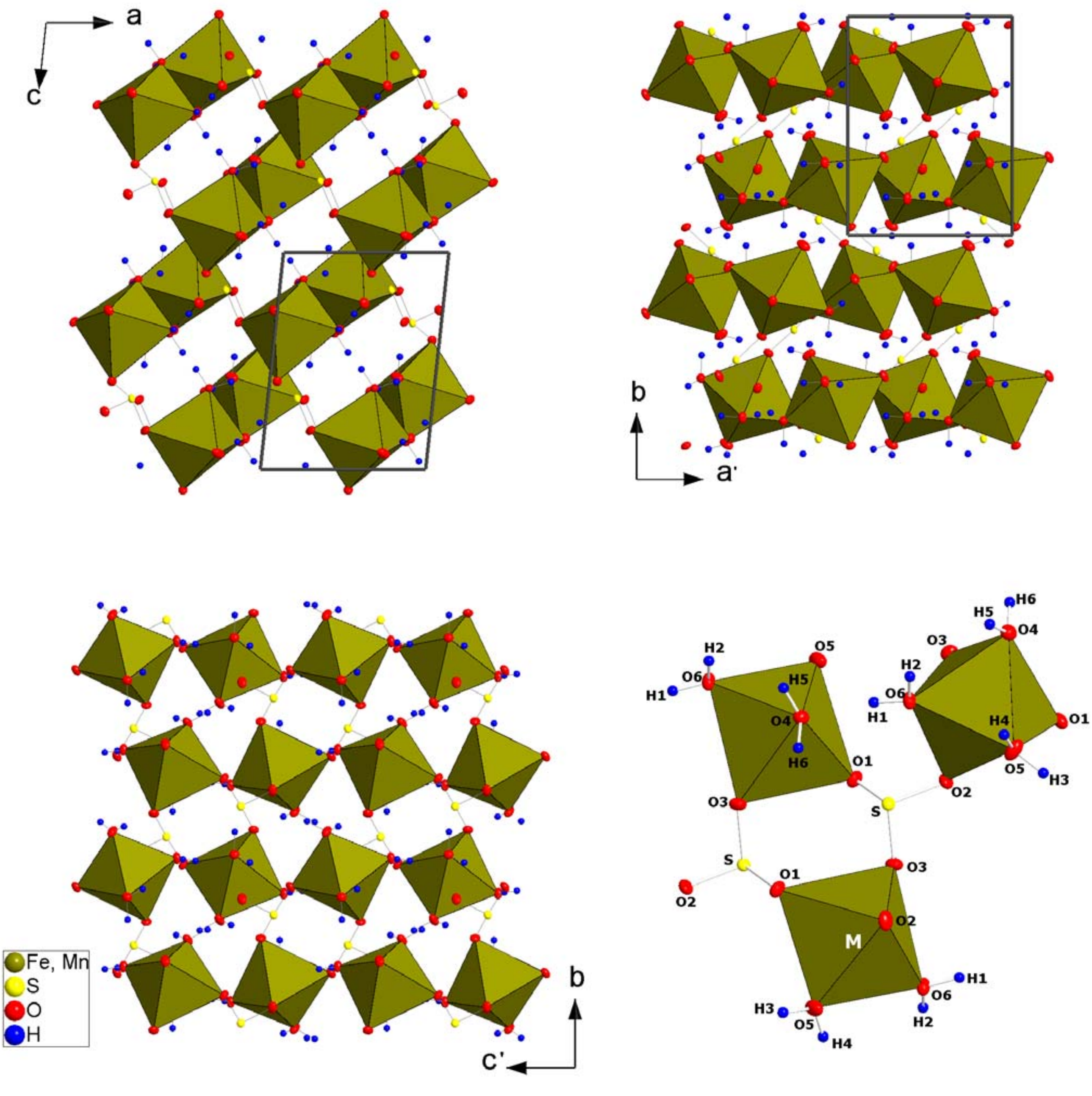
a
c
b
a'
Fe, Mn
S
O
H
b
c'
H2
O6
H1
O5
H5
O4
H6
O1
O3
S
O2
H6
H5
O4
O3
H2
O6
H1
O1
H4
O5
H3
O2
S
O1
O3
O2
M
H1
O6
H3
O5
H2
H4